A comparative study of heavy metals removal using agricultural waste biosorbents

Begum Tokay* and Isil Akpinar

Chemical and Environmental Engineering Department, Faculty of Engineering, University of Nottingham, University Park, Nottingham NG7 2RD, UK

**corresponding author: begum.tokay@nottingham.ac.uk*

Abstract

The adsorption capabilities of rice husk, coconut coir and moringa seeds were evaluated for the first time under the same experimental conditions for the removal of copper (Cu), nickel (Ni) and zinc (Zn from underground water. The effects of adsorbent dosage, pH and contact time were studied. Copper and nickel were removed up to 99%, using rice husk, coconut coir and moringa seeds. Zinc concentrations can only be reduced to up to 70% using rice husk. However, removal was reached 99% when coconut coir and moringa seeds were used. Moring seeds showed the highest adsorption capacities (Zn= 42.3 mg g^{-1}, Cu= 23.3 mg g^{-1}, Ni= 16.1 mg g^{-1}) amongst the biosorbents tested. Nickel was the least adsorbed heavy metal for all biosorbents studied. Moringa seeds leached sulfur at acidic pH values (< 4). Models showed that adsorption using these biosorbents follows Langmuir isotherm and Pseudo-second order kinetic.

Keywords: rice husk; coconut coir; moringa oleifera seeds; heavy metal removal; adsorption; biosorbents

1. Introduction

Water pollution is a global challenge and causes health problems throughout the world (Bakker, 2012). The contaminated water with heavy metals is known to be an environmental issue and have a significant effect, particularly on the developing countries. Industrial processes such as metal plating, fertilizer production, barrier fabrications, smelting and mining operations (Peng et al., 2018), have greatly enhanced the mobilisation of the heavy metals. Hence, they are entering directly or indirectly into the environment by means of various sources. They have

threatened to aquatic organisms and human life as they are known to be toxic or carcinogenic (Fu and Wang, 2011). Although several heavy metals, such as zinc (Zn), iron (Fe), manganese (Mn) and cobalt (Co), have an important role in biochemical processes in human body, they are highly toxic as ions or in compound forms; they are soluble in water and may be readily absorbed into living organisms. (Abdullah et al., 2019). Heavy metals of particular concern in treatment of industrial wastewaters include zinc, copper, nickel, mercury, cadmium, lead and chromium. Therefore, the mitigation of these heavy metals is of utmost significance. Too much zinc can cause health problems, such as stomach cramps, skin irritations, vomiting, nausea and anemia (Oyaro et al., 2007). Excessive ingestion of copper causes e.g. vomiting, cramps, convulsions, or death (Paulino et al., 2006). High nickel levels may result serious lung and kidney problems aside from gastrointestinal distress, pulmonary fibrosis and skin dermatitis (Borba et al., 2006).

There are various treatment methods, such as membrane technology (Abdullah et al., 2019), precipitation, coagulation-flocculation, ion exchange and adsorption, have been implemented to treat these heavy metals from wastewater and water (Abdullah et al., 2019). These methods have some drawbacks, including high energy cost, inefficient removal, production of toxic sludge and fouling of metal ions (Sun et al., 2018). However, adsorption-based technologies have potential to remove heavy metal ions due to their simplicity and cost efficiency (Peng et al., 2018). A wide range of adsorbents, such as activated carbons (Kołodyńska et al., 2017), clays (Seliman et al., 2014), zeolites (Lu et al., 2016) and metal-organic frameworks (Mon et al., 2016) , have been studied for the heavy removal from water. In adsorption-based technologies, low-cost and environmentally friendly alternative sorbents are still needed to be explored e.g., biosorbents, which are produced from agricultural waste. Biosorbents that are available in nature and prepared from agro-wastes such as rice husk (Shukla, 2008), coconut coir (Asim et al., 2020), maize straw (Guo et al., 2015), orange peel

(Gupta & Nayak, 2012) and moringa oleifera seeds (Obuseng et al., 2012;) have been used with or without chemical modifications. In these studies, biosorbents were investigated for the removal of lead (II), copper (II), zinc (II), manganese (II), nickel and arsenic from water. These cost-effective and environmentally benign materials have exhibited effective removal of heavy metals and thus are considered as sustainable sorbents used for heavy metals in water treatment (Mohan and Sreelakshmi, 2008). Zhang et al (2014) determined the Cu adsorption capacity of rice husk that they reported 89% removal and 17 mg g^{-1} adsorption capacity. In contrast, Marshall et al (1993) reported relatively low adsorption capacities for Cu (1.21 mg g^{-1}), Zn (0.75 mg g^{-1}) and Ni (0.23 mg g^{-1}) using rice hulls and bran, which could be resulted from multi-component adsorption effect and biosorbent properties. Studies using coconut coir for adsorption of heavy metals are limited. Aravind et al (2017) reported up to 90% Ni and Cu removal (from Ni= 5 mg l^{-1}, Cu=5 mg l^{-1} and Cd= 0.9 mg l^{-1} initial solution). Abdul Rahil et al (2020) estimated the adsorption capacities for Cu and Ni approx. 0.15 mg g^{-1} and 0.05 mg g^{-1}, respectively, using coconut waste-based adsorbent. Performance of moringa seeds for heavy metal removal were also studied. Obuseng et al (2012) showed that unmodified moringa oleifera seeds can remove 5 mg l^{-1} Cu, Zn and Ni from water up to 80%, 60% and 20%, respectively, in an hour. Similarly, Maina et al (2016) reported up to 60% and 40 % removal for Zn and Cu from multi-element solution. They also concluded that the pH, initial metal concentration, biosorbent amount, particle size, and temperature affected the adsorption process.

In this study, we explored the feasibility of using natural sorbents such as coconut coir, rice husk and moringa seeds, for heavy metal removal, particularly copper, zinc and nickel, from water. For the first time, these biosorbents were compared using the same initial heavy metal concentrations, simulating heavy metals mixed in underground water sources. The influences of adsorbent amount, solution pH and contact time on their adsorption capacity

towards mixed heavy metals were elucidated. Adsorption isotherms and kinetics were determined. Biosorbents were also characterised using multiple techniques, including X-ray diffraction (XRD), scanning electron microscopy (SEM), Fourier transform infrared spectroscopy (FTIR) in order to explain heavy metal removal mechanism.

2. Experimental

Biosorbent preparation

Asian rice husk was purchased from Thailand (T.K. Rice Mill, Bangkok). After crushing (Retsch Mill SM2000) and sieving (250 μm), samples were washed thoroughly for 15 minutes to remove any dirt and metals that could interact with the main experiments. The samples were dried in an oven at 50 °C for 24 hours and then stored in polythene bags in a desiccator at room temperature (RT) to avoid any increase in moisture content.

The coconut coir pith was purchased from Exotic Pets in the form of dense brick. Samples were shredded using a Retsch Mill SM2000 and sieved to obtain average particle size of 500 μm. They were washed thoroughly, dried at 90 °C in a conventional oven overnight and then stored in polythene bags in a desiccator at room temperature.

The moringa oleifera seeds used in the experiment was supplied from Seeds-Store, Germany (harvested in Egypt/Canary Islands). The dark-brown shells were manually cracked in order to remove the kernels. The small and white seed kernels were shredded using a Retsch M2000 Shredder. The powder was sieved in the range of 710-850 μm, resulting with an average particle size of 783 μm. Samples were then stored in polythene bags in a desiccator at room temperature.

Characterisation of biosorbents

X-ray diffraction (XRD) measurement was performed using a PANanalytical X'Pert Pro diffractometer operating at 40 kV, 40 mA and CuKα radiation (λ: 1.540598 Å), equipped with a PIXCell3D detector. The scan was obtained between 10-70^{o} (2θ).

The morphology of the biosorbents were characteristics by scanning electron microscopy (SEM, JEOL JSM-7100F). The samples were coated with 10-20 nm thick gold layer before analyses. Imaging was conducted at 5 kV.

The functional groups present in the biosorbents were characterized by a Fourier transform infrared (FTIR) spectrometer (Bruker IFS66) using diffuse reflectance mode. The spectral range was varied from 4,000 to 400 cm^{-1}. All the spectra were obtained under absorbance mode.

A Panalytical Epsilon 3XL model X-ray fluorescence analyser (XRF) was used in determining both the qualitative and quantitative elemental composition of the samples. Powder samples were placed in a plastic cup to about 4.9 cm in depth and covered with a plastic film at the bottom. Approximately, 5 g of powder was used during measurements.

Zeta potential of samples (at pH 7) was determined using A Zetasizer Nano ZS instrument (Malvern, UK). The pH was adjusted to 7 by mixing 0.25 g of biosorbent, 1 g of NaCl, 100 ml of distilled water, and 1-2 ml of 0.5 M NaOH.

Specific surface area of biosorbents were estimated using nitrogen adsorption-desorption isotherm measurements (Micrometrics 3Flex adsorber). Dried samples were degassed for 3 h at 150 ^{o}C before analysis and cooled to -196 ^{o}C using liquid nitrogen. The distribution of micropores was analysed by the *t*-plot method.

Heavy metal solution preparation

Multi-component solutions of Cu, Zn and Ni were freshly prepared prior to each adsorption experiment to simulate the water sources. For adsorption tests, brackish water solutions were obtained by dissolving sodium chloride (NaCl), copper (II) chloride dihydrate ($CuCl_2.2H_2O$), zinc sulfate heptahydrate ($ZnSO_4.7H_2O$) and nickel (II) nitrate hexahydrate ($Ni(NO_3)_2 \cdot 6H_2O$) in water purified using Milli-Q®-IQ 7015 Ultrapure lab water purification

system (at 18.2 MΩ.cm resistivity). All chemicals were purchased from Sigma-Aldrich and used without further treatment.

Quantitative analysis of heavy metal concentrations in water

For analyses using inductively coupled plasma atomic emission spectroscopy (ICP-AES, Perkin Elmer 300 DV), around 25 ml of samples was taken from the solutions at predetermined times. The adsorbents were separated from solutions *via* centrifugation (Hettich, Rotofix 32 A) at 3,000 rpm for 5 min. The supernatant was decanted and passed through a Minisart® (0.45 μm, hydrophilic) syringe filter. A 10 ml aliquot of the filtered solution was then pipetted in a 15 ml polypropylene conical tube and the sample was acidified with 5 ml of 30% (v/v) nitric acid and refrigerated to prevent metal precipitation and microbial degradation.

Calibration standards were prepared by using a multi-element solution. Three-point calibration curves were established for each metal species. For quality control, ultrapure water sample (18.2 MΩ.cm resistivity) was included in every batch of analysis.

Adsorption experiments

Batch adsorption studies were conducted at room temperature (21 ± 3 °C) using 400 ml of heavy metal solution. Solutions were continuously stirred at a constant rate using a magnetic stirrer. The details of the initial contaminant concentrations and experimental conditions are given in Table 1.

Table 1. Initial concentrations of heavy metals and experimental conditions.

Biosorbents	Contaminants	Concentration of Adsorbents in Water ($g\ l^{-1}$)	Initial Concentration of the Contaminants ($mg\ l^{-1}$)	pH
Coconut Coir	Copper	2, 5, 10, 20, 40	2.9	6
	Zinc	2, 5, 10, 40	0.84	
	Nickel		0.174	
Rice Husk	Copper		2.9	6

	Zinc	2, 5, 10, 40	0.84	
	Nickel		0.174	
Moringa Oleifera	Copper	2, 5, 10, 40	2.9	6
	Zinc		0.84	
	Nickel		0.174	

The effect of precipitation was quantified by control experiments where pH of the solution was adjusted to 3.5, 6.5 and 10.5 with mixed heavy metal solutions without biosorbents. The heavy metal concentrations were set to 1 mg l^{-1} and 12.5 mg l^{-1} and initial/final concentrations of heavy metals were measured. During the adsorption experiments, pH was continuously monitored and adjusted by adding 5 M NaOH and/or HCl dropwise to the working solution under vigorous stirring and using a Hanna HI 5522-02 pH-meter, which was calibrated daily using fresh buffer solutions. No more than 4 ml of 5 M NaOH and/or HCl were needed to adjust the pH to a desired value in all the experiments. The effect of pH on the uptake of copper using rice husk, coconut coir and moringa seeds was also studied at the pH values of 4, 6, 8 and 10 at a constant adsorbent dosage (10 g l^{-1}) for 2 h. This is because copper solubility in water dramatically reduces from 20 to 0.05 mg l^{-1} between pH 6-8 hydroxide (https://heienv.com/hydroxide-precipitation-of-metals/)

To determine the adsorbent dosage and contact time for the adsorption tests, 2-40 g l^{-1} of coconut coir, rice husk and moringa seeds were added to the water samples (at optimum pH determined) and solutions were mixed on a magnetic stirrer. Adsorption isotherms were constructed using 40 g l^{-1} biosorbents with the heavy metal concentration range of 1-150 mg l^{-1} at pH 6.

Sulfur leaching rate from moringa oleifera seeds (5 g l^{-1}) was also studied at various pH values (4-7) up to 120 minutes. Sampling from water solutions and metals analysis were performed, as explained previously.

Removal efficiency as percentage and adsorbed amount of metals were calculated using the following equations, respectively.

$$\mathrm{Re}\ (\%) = \frac{(C_0 - C_e)}{C_0} \times 100 \quad (1)$$

$$Q_e = \frac{(C_0 - C_e)\,V}{m} \quad (2)$$

where, R_e is removal efficiency (%), C_0 is the initial concentration (mg l^{-1}), C_e is the residual concentration (mg l^{-1}) at equilibrium, V is the volume of the solution and m is the adsorbent dosage (g).

The adsorbed amount on the biosorbents were calculated by using the mass-balance relationship, which is given in the following equation.

$$Q_t = (C_0 - C_t) \times \left(\frac{V}{m}\right) \quad (3)$$

where, Q_t (mg g^{-1}) is the amount adsorbed per unit mass of adsorbent in time t (min), C_o (mg l^{-1}) is initial liquid-phase concentration of adsorbates at time equals to 0, C_t (mg l^{-1}) is liquid phase concentration of heavy metals at time equals to t (min), V (l) is the volume of the solution and m (g) is the mass of the biosorbent.

$$\ln(Q_e - Q_t) = \ln(Q_e) - k_1 \times t \quad (4)$$

$$\frac{t}{Q_t} = \frac{1}{k_2 \times {Q_e}^2} + \frac{1}{Q_e} \quad (5)$$

where, Q_t (mg g^{-1}) and Q_e (mg g^{-1}) are the adsorbed amount of metal ions at time t (min) and at equilibrium, respectively; k_1 (min^{-1}) is the pseudo first order rate constant and k_2 (g mg^{-1} min^{-1}) is the pseudo second order rate constant and t (min) is the adsorption time.

To determine the adsorption mechanism, Freundlich (Eq 6) and Langmuir (Eq 7) models were employed that are given by the following equations:

$$Q_e = K_F . C_e^{\frac{1}{n}} \quad (6)$$

where K_F is the constant of Freundlich isotherm indicating the adsorption capacity of the biosorbent, C_e is the adsorbate concentration in the solution at equilibrium and 1/n is a representation of the adsorption intensity between the biosorbent and adsorbate molecules.

$$\frac{C_e}{q_e} = \left(\frac{1}{bq_m}\right) + \frac{C_e}{q_m} \quad (7)$$

where, C_e is the adsorbate concentration in the solution at equilibrium, q_e is the amount of solute adsorbed per unit mass of biosorbent, b is the constant of Langmuir isotherm and q_m is the maximum adsorptive capacity of the biosorbent at equilibrium.

Results and Discussions

Characterisation

The crystal structure of the biosorbents were evaluated using XRD. A broad reflection was detected at the 2θ of 22.5º for rice husk that is a characteristic peak of amorphous silica (Seliem et al., 2016). The XRD pattern of moringa seeds showed a broad band approx. at the 2θ of 20º, which is attributed to the amorphous nature of the material. This is due to the high composition of protein and oil (Abdulkarim et al., 2005). Araújo et al (2010) suggested the adsorbate can more easily penetrate the surface of the adsorbent, thus favouring the adsorption process because of the amorphous nature of the adsorbent. XRD pattern of the coconut coir also showed low crystallinity (amorphous). The amorphous characteristic of the coir is due to the high lignin content in its structure (Rosa et al., 2010). The peaks ~ 16º, 22º and 35º represent cellulose (Tomczak et al., 2007).

The structures of of rice husk, coconut coir and moringa seeds were investigated via SEM. The irregular superficial layer of silica and natural resins can be observed in rice husk structure. Coconut coir pieces approx. 25 micron in size with the small entities on the surface of the large pieces. The seeds of the Moringa oleifera is visible whilst they are agglomerated and grouped together, resulting up to 50 micron in size.

The functional groups were determined in order to understand the interaction between the biosorbents and the metal ions using FTIR. The broad peak that was observed approx. at 3340 cm^{-1} for all 3 biosorbents indicates strong O-H (H-bonded) stretching of cellulose and lignin in macromolecular association (Tariq et al., 2018). The peak at 1060 cm^{-1} represents OH

group, which is derived from deformation modes of alcohol or phenol, with a sterically hindered OH and also represents functional groups of Si–O–Si (Pathiraja et al., 2014). The small peak observed at 1254 cm^{-1} for coconut coir possibly represent C-C and C-O and stretching and COH bending at C6 in cellulose (Sangian et al., 2017) The FTIR spectra of moringa seed showed the presence of various functional groups, compared to rice husk coconut coir. The bands in approx. 2920 cm^{-1} and 2854 cm^{-1} in moringa seeds were attributed to the symmetric and asymmetric stretching of group C-H-CH_2 present in fatty acids (Araújo et al., 2010). Two strong absorption bands were observed at 1654 cm^{-1} and 1546 cm^{-1} that are characteristics of amide I and II respectively, which confirms the structure of the protein present in moringa seeds. The peak at 1747 cm^{-1} belongs to the carbonyl (C=O) stretching vibration of the carboxyl groups of lignin in the moringa seeds (Feng et al., 2009).

BET surface areas, estimated pore diameters and zeta potentials of the biosorbents are shown in Table 2. Moringa seeds and coconut coir have 2 times higher BET surface area than rice husk. However, results showed that the surface area of these biosorbents are much smaller (< 19 $m^2\ g^{-1}$) than other adsorbents. Rice husk and moringa seeds have micropores (< 2 nm) while coconut coir has mesopores (2-50 nm). In agreement with the literature result, these biosorbents are negatively charged at pH 7, observed by zeta potential measurements (O' Bezerra et al., 2018).

Table 2: BET Surface area, estimated pore diameter and zeta potential of biosorbents

Biosorbent	BET surface area ($m^2\ g^{-1}$)	Pore diameter (nm)	Zeta potential (mV)*
Rice husk	8.1 ± 0.1	1.5	-38.2 ± 0.2
Moringa seed	18.9 ± 0.2	1.6	-28 ± 0.012
Coconut coir	16.7 ± 0.3	3.9	-22 ± 0.5

*pH= 7, T= 25 ^oC

The chemical compositions of biosorbents used in this study are presented in Table 3. Quantitative analysis using XRF showed that rice husk mainly constitutes Si (94 mg g^{-1}). The

Si contents of coconut coir and moringa seeds are ~13.6 mg g^{-1} while moringa seeds also contain K (16.9 mg g^{-1}). All three biosorbents' Al content is similar (10.4 mg g^{-1}).

Table 3: Elements obtained in the biosorbents via XRF analysis.

Biosorbent	Al (mg g^{-1})	Si (mg g^{-1})	K (mg g^{-1})	Ca (mg g^{-1})
Rice husk	10.4 ± 0.4	94.0 ± 3	5.6 ± 0.2	1.7 ± 0.1
Moringa seeds	10.5 ± 0.2	13.6 ± 0.3	16.9 ± 0.4	4.1 ± 0.01
Coconut coir	10.5 ± 0.4	13.5 ± 0.2	3.2 ± 0.4	0.25 ± 0.14

Adsorption experiments

Table 4 shows the effect of pH on the precipitation of the heavy metals. There is no significant precipitation of heavy metals at pH 4 and 6 for both initial concentrations. The precipitation of copper and zinc started at pH 8. All three heavy metals precipitated at pH >10 due to an increase in metal hydroxide formation that is insoluble. Copper's theoretical solubility is 20 mg l^{-1} at pH 6. This reduces to 0.05 mg l^{-1} at pH 8. Nickel's solubility has a similar trend, but drastic reduction occurs after pH ~9 (Solubility 70 mg l^{-1} and 0.1 mg l^{-1} at pH 8 and 10.2, respectively). Zinc's solubility has a minimum (0.1 mg l^{-1}) at pH ~10.5. These results suggest that adsorption experiments can be conducted at pH 4 or 6 to avoid precipitation.

Table 4: Precipitation of heavy metals as a function of pH (4, 6, 8, 10) Initial metal concentrations are ~ 1 and ~12.5 mg l^{-1} for each heavy metal (T= 20 ± 2 °C).

pH	Time (h)	Cu (mg l^{-1})		Zn (mg l^{-1})		Ni (mg l^{-1})	
4	0	1.1	12.5	1.1	12.6	1.1	12.5
	2	0.99	12.3	0.98	12.2	0.97	12.4
6	0	1.1	12.6	1.1	12.6	1.1	12.5
	2	0.95	9.8	0.99	12.4	0.98	12.3
8	0	1.1	12.4	1.1	12.4	1.1	12.4
	2	0.012	0.056	0.009	8.4	0.99	12.2
10	0	1.1	12.6	1.1	12.6	1.1	12.5
	2	0.005	0.009	0.004	0.0085	0.045	0.093

The copper concentration as a function of pH using rice husk were given in Figure 1. The copper removal with adsorption increased by approx. 55% when the pH value was

increased from 4 to 6. In contrast, the reduction in copper concentration occurred at pH 8 and 10 was due to chemical precipitation rather than adsorption. The optimal pH value was determined as 6 for the adsorption of Cu on rice husk, showing the highest removal (75%). That is approx. three times greater than the copper removal by adsorption at pH 4. Therefore, the rest of the experiments using rice husk was performed at pH 6.

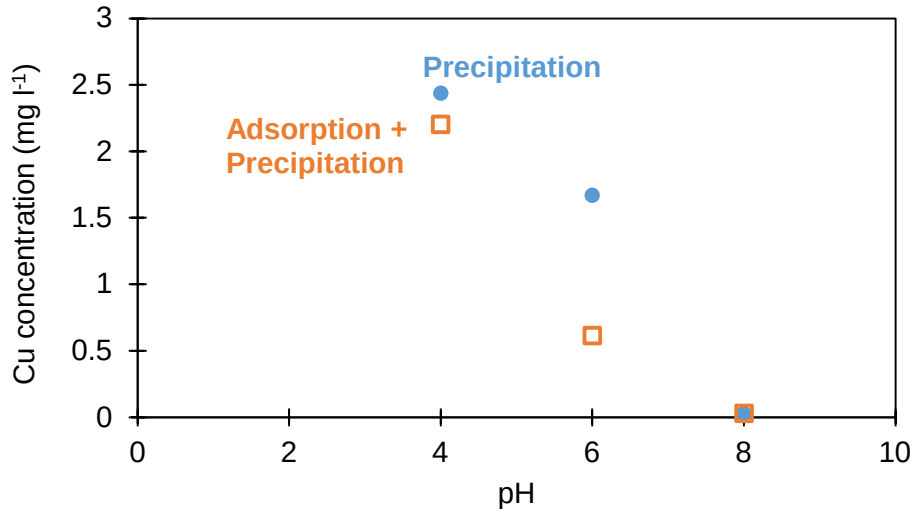

Figure 1. The effect of pH on the copper removal by precipitation and adsorption using rice husk. (Rice husk amount=10 g l^{-1}, Temperature = 21 ± 3 °C, and initial Cu concentration = 2.9 mg l^{-1}, ± error < 2%).

Figure 2 shows the Cu, Zn and Ni concentrations in water as a function of contact time at a range of rice husk dosages (2-40 g l^{-1}) at room temperature. The concentration of Cu and Zn dropped drastically within the first 5-15 minutes. This can be attributed to the availability of the abundant active sites on the surface of rice husk (Zhang et al., 2014). For all the rice husk dosages investigated, the optimum contact time for Cu was observed approx. 2 hours as the percentage removal did not increase significantly beyond this time (Fig 5). A maximum removal percentage of Cu (98%) was achieved at 2 hour of contact time with 40 g l^{-1} rice husk. It is worth noting that around 75% of Cu was removed within the first 5 minutes using 40 g l^{-1} rice husk. Although up to 70% of Zn was removed at 2 hour of contact time using 40 g l^{-1} rice husk, the saturation was reached after 6.7 hours. Removal percentage of Zn increased from 16 to 32, when 5 and 10 g l^{-1} adsorbent used during the experiments. Approximately 98% of Ni

was removed using 40 g l^{-1} of rice husk at pH 6 in 2 hours. Similarly, saturation was obtained ~ 7 h where up to 45% Ni was removed. These saturation times for Zn and Ni may suggest that adsorption of Zn and Ni on rice husk is slower than that of Cu.

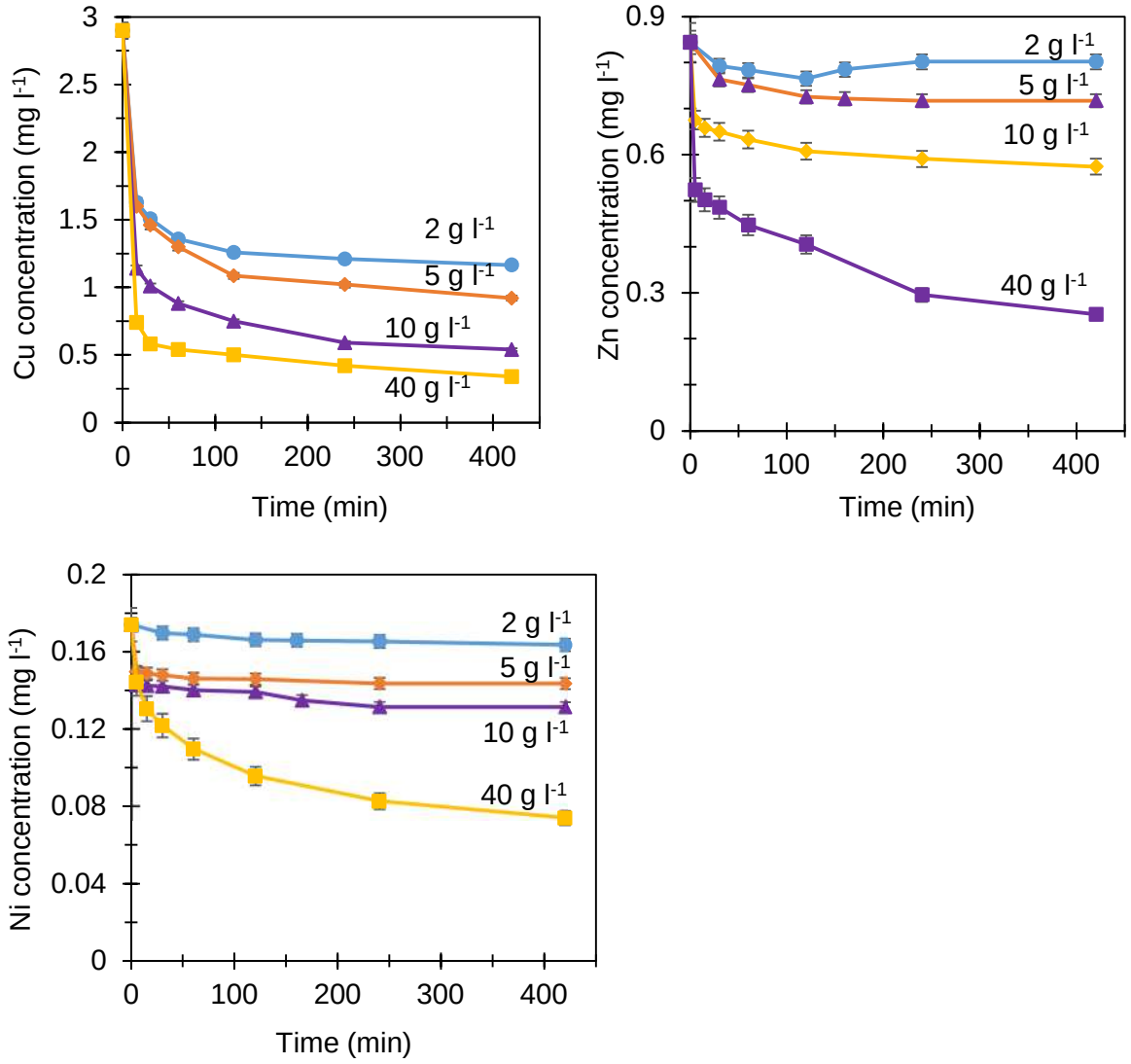

Figure 2. The concentrations of Cu, Zn and Ni in water as a function of time for rice husk dosages of 2-40 g l^{-1} at pH 6 (± error < 5%).

The main factor contributing to the adsorption properties of the rice husk is the presence of silanol functional groups on its surface, which is related to its silica content that can reach up to 20 wt% (Ahmaruzzaman and Gupta, 2011). The porosity of the rice husk is low (Table 3) and the main functional group present in the structure is Si-O-Si bonds as observed by FTIR spectra (Fig 3). Negative surface charge of rice husk is also one of the factors contributing to

adsorption of positively charged heavy metals on the surface. In addition to this, cellulose and lignin components can also play role of the removal of the heavy metals [Rocha et al., 2009]

Figure 3 represents the removal of copper by adsorption and precipitation as a function of pH using 10 g l^{-1} coconut coir for 2 hours. At pH 4, the copper concentration only decreased to 2.25 mg l^{-1} (33% removal) while up to 92% of copper was removed at pH 6. The copper concentration at pH 8 and 10 decreased below the detection limit (0.013 mg l^{-1}) of the ICP-AES (Figure 6). These suggests that the copper removal using coconut coir significantly increased at pH values > 6 due to the precipitation. Therefore, the rest of the adsorption experiments of Cu on coconut coir were conducted at pH 6, showing the highest removal efficiency of 92%. These observations coincide with the results published for copper adsorption on coconut coir (Kadirvelu & Namasivayam, 2003) and the greater removal by adsorption and predominantly by precipitation was observed at pH > 6.

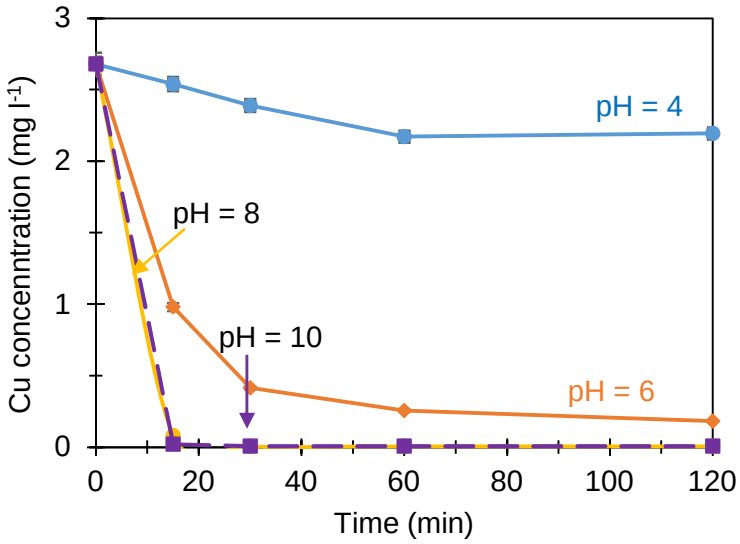

Figure 3. The effect of pH on the copper removal by adsorption and precipitation as a function of time (Coconut coir amount= 10 g l^{-1}, initial concentration of Cu= 2.9 mg l^{-1}, ± error < 3%).

The uptake of copper increased when the coconut coir dose was increased in the range of 2-40 g l^{-1} (Figure 4). Most of the copper was removed within the first 5 minutes whilst concentrations decreased until 2 h. Almost 85% of the copper in water was removed at pH 6, using 10 g l^{-1} of coconut coir within 120 minutes. When the coconut coir concentration was

305 increased to 40 mg l^{-1}, the copper concentration dropped to 0.0065 mg l^{-1}. Unlike rice husk, 2
306 g l^{-1} coconut coir can remove approx. 53% of all the heavy metals. Percentage removal are
307 similar to rice husk results for Zn (86%) and Ni (89%) using 10 g l^{-1} of coconut coir. Up to
308 99% removal was achieved for all heavy metals when the coconut coir amount was increased
309 to 40 g l^{-1}. These results may indicate that Cu is adsorbed more by rice husk whilst coconut
310 coir adsorbs more Zn and Ni. The differences in surface area and functional groups affect the
311 adsorption properties of the biosorbents. The BET surface area and pore size of coconut coir
312 are approx. 2 times higher than rice husk. The functional groups that belong to cellulose in
313 coconut coir may also play a role during adsorption more than surface charges as both
314 biosorbents are expected to be negatively charged at pH 6.

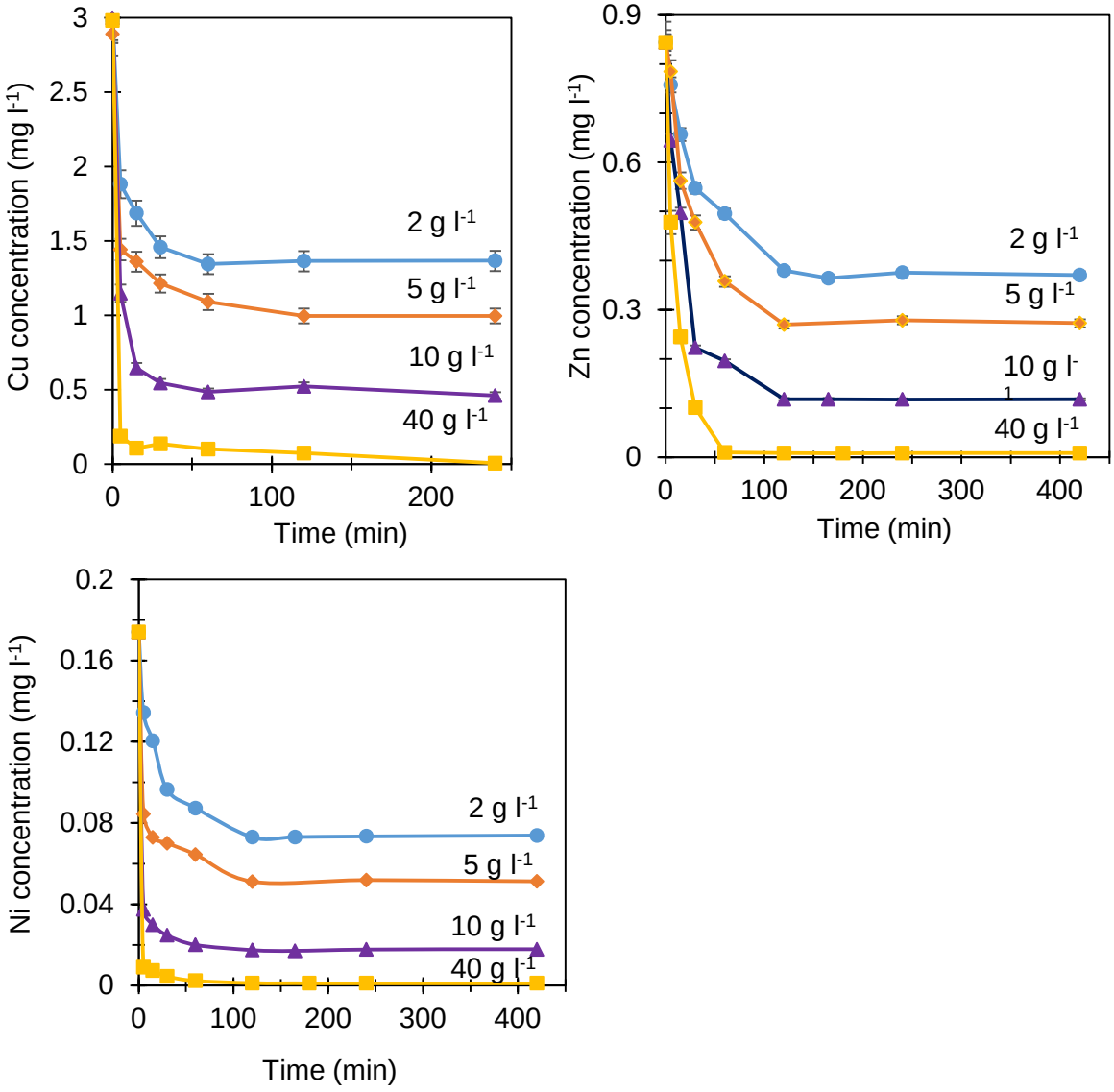

Figure 4. The concentrations of Cu, Zn and Ni in mixed heavy metal solution as a function of time for coconut coir amounts of 2-40 g l^{-1} at pH 6 (± error < 5%).

The concentrations of Cu, Zn and Ni in mixed heavy metal solution as a function of time for moringa seeds are shown in Figure 5. Only 2 g l^{-1} moringa seeds are sufficient to remove 90%, 85% and 80% of Zn, Cu and Ni, respectively, in 30 min. With increasing biosorbent dose (40 g l^{-1}), 99% removal was achieved for all heavy metals.

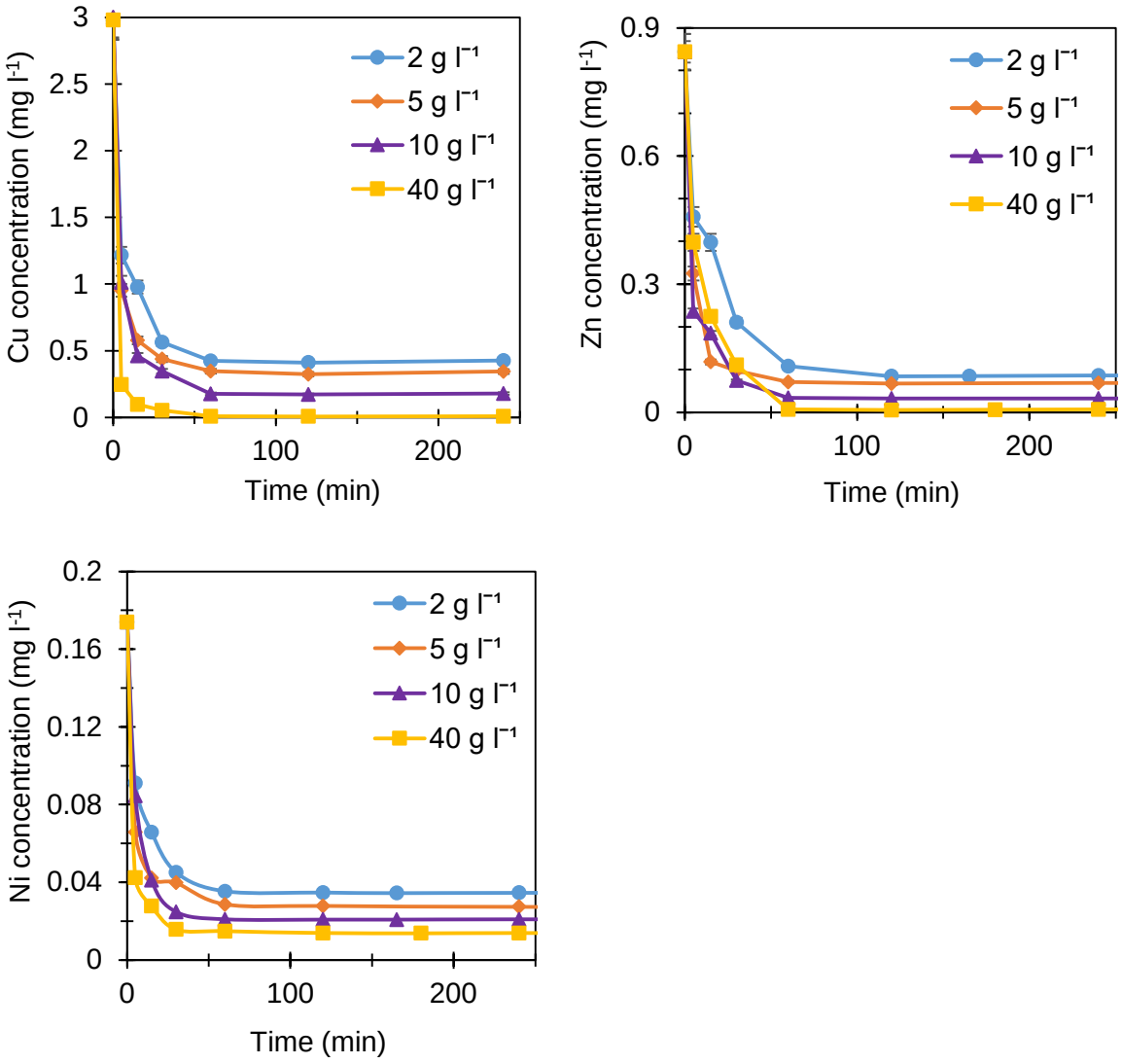

Figure 5. The concentrations of Cu, Zn and Ni in mixed heavy metal solution as a function of time for moringa seeds amounts of 2-40 g l^{-1} at pH 6 (± error < 5%).

These results may suggest that moringa seeds are convenient biosorbent for the removal of Zn, Cu and Ni without multi-element effect, mostly seen during adsorption processes. Regarding the FTIR spectra, moringa seeds contain more functional groups than the other two biosorbents used in this study. This may be the reason of better removal obtained. In addition to this Bhatti et al (2007) reported an optimal pH range (5-8) for heavy metal removal using moringa oleifera seeds. Similarly, Araújo et al (2010), showed 80, 60, 20% Zn, Cu and Ni removal efficiency, respectively at the pH range of 4-6.

A qualitative analysis of the treated water samples during the adsorption experiments showed considerable amounts of sulfur being leached into the water (Figure 6). Due to the potential health effects and colour and odour issues, sulfur leaching at various pH values were further studied. The value of pH had a strong effect on the rate at which sulfur leached to the aqueous solution, with higher acidity promoting the sulfur leaching. During the experiments, the highest sulfur concentration (100 mg l^{-1} ± 3) was measured at pH 4. In contrast, for pH 6 and 7, the sulfur concentrations were approximately 40 mg l^{-1} ± 2.

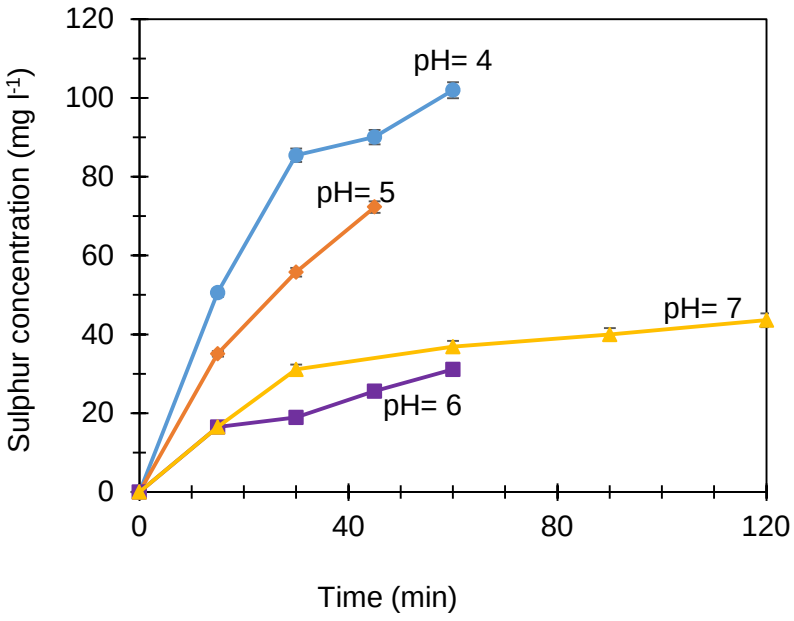

Figure 6. Increase in sulphur concentration as a function of time (pH=4-7, dosage= 5 g l^{-1}).

The leaching of sulfur from seeds may be attributed to the stronger competition between H^+ ions and sulfur molecules at low pH values. No reporting of similar occurrences has been published in literature; therefore, no data is available for comparison. There are no limits imposed on elemental sulfur, sulfate or hydrogen sulphide in drinking water regulation. However, the World Health Organisation reported that laxative effects of sulfate was observed when water with concentrations of sulfate above 1000 mg l^{-1} was consumed (WHO, 2004). The taste threshold is also indicated as 250 mg l^{-1} for sodium sulfate. Assuming most of the sulfur detected by the ICP-AES instrument is present in water as sodium sulfate, the taste threshold

of 250 mg l^{-1} corresponds to approximately 50 mg l^{-1} of sulfur. As shown in Figure 6, the calculated threshold would not be exceeded when operating at pH 6 and 7, whereas for pH values of 4 and 5, the contact time will have to be limited at 30 minutes and 15 minutes, respectively.

Adsorption kinetics of Cu, Zn and Ni

To determine the adsorption kinetics of Cu, Zn and Ni using rice husk, coconut coir and moringa seeds, the samples were taken at specified times. Furthermore, the adsorbed amount values and the kinetic parameters were demonstrated using the linearized forms of the two kinetic models by fitting with the experimental data. As the pseudo-second order model best fitted the kinetic data ($R^2 > 0.99$) for all heavy metals using rice husk, coconut coir and moringa seed (Table 5). The first-order model produced low regression coefficients, indicating a weak correlation between this model and the experimental data. Therefore, only the results from the pseudo-second order model are presented in Table 5. These results are in agreement with the reports published in literature for rice husk (Zhang et al, 2014) and coconut coir (Shukla et al., 2006; Fu and Wang, 2011). The moringa seeds kinetic study has not published for the heavy metals investigated in this study. However, Kalavathy and Miranda (2010) reported that adsorption of Cu, Zn and Ni follow pseudo- second order kinetic model using moringa oleifera wood. Similarly, Ni adsorption on moringa oleifera seed husks followed pseudo-second order kinetics (Garcia-Fayos et al., 2015).

Table 5: Pseudo-second order model kinetic parameters for Cu, Zn and Ni adsorption on rice husk, coconut coir and moringa seeds at pH 6 using 5 g l^{-1} biosorbent.,

Biosorbent	Metal ion & initial concentration (mg l^{-1})	k_2 (g mg^{-1} min^{-1})	$Q_{e\ (calc)}$ (mg g^{-1})	R^2
Rice husk	Cu, 3	0.19	0.41	0.9997
Coconut coir		0.6	0.38	0.9994
Moringa seeds		0.641	0.535	0.999

Rice husk	Zn, 0.844	6.57	0.0257	0.995
Coconut coir		0.0966	0.139	0.956
Moringa seeds		1.69	0.157	0.999
Rice husk	Ni, 0.174	12.3	0.0085	0.993
Coconut coir		12.6	0.0247	0.999
Moringa seeds		7.74	0.03	0.999

Moringa seeds exhibited the highest equilibrium capacities (Q_e) and pseudo-second order rate constant (k_2) for Cu. Although the equilibrium capacities of Zn (0.157 mg g^{-1}) and Ni (0.03 mg g^{-1}) were also the highest for moringa seeds, pseudo-second order rate constants (k_2) for Zn and Ni were the highest when rice husk and coconut coir were used.

Studies have shown that adsorption behaviour that fits the second order kinetic model well often can be explained by diffusion-based mechanisms. Therefore, adsorption kinetics of cellulosic materials may mainly depend on diffusion-limited processes, as affected by heterogeneous distributions of pore sizes and continual partitioning of solute species between a dissolved state and a fixed state of adsorption, as discussed previously (Douven et al, 2015). Alternatively, some studies concluded that the pseudo-second order model suggests either a chemisorption or an ion-exchange mechanism, depending on the functional group of the adsorbent (Blanchard et al., 1994). Since these biosorbents have low BET surface area (Table 3), in order words not very porous, diffusion of heavy metals may be critical only in the solution while they are attracted to the surface of biosorbent through weak Van der Waal's forces (electrostatic attraction). Rudi et al., 2020 suggested that the chemical bonds between the metal ions and the rice husk surface occurred during adsorption. Therefore, Ahmaruzzaman and

Gupta (2011) emphasised the importance of improving the properties of the rice husk surface since the adsorption properties of the material could be enhanced.

Adsorption isotherm models

Langmuir model well-fitted the adsorption data obtained for 3 heavy metal ions using rice husk, coconut coir and moringa seeds since regression coefficients (R^2) are in the range of 0.98-0.99 (Table 6). Freundlich model was also applied in describing adsorption isotherms for Cu, Zn and Ni that fit with lower regression coefficients (R^2= 0.88-0.90) and thus was not shown in Table 6.

Table 6: Langmuir adsorption isotherm model parameters for Cu, Zn and Ni using rice husk, coconut coir and moringa seeds as biosorbents. Adsorbent dose: 40 g l-1, Heavy metal concentration: 1-150 mg l^{-1}, pH=6

Biosorbent	Parameter	Cu	Zn	Ni
Rice husk	q_{max} (mg g^{-1})	1.56	0.89	0.64
	b (l mg^{-1})	3.7	24.0	65.8
	R^2	0.9986	0.9878	0.9966
Coconut coir	q_{max} (mg g^{-1})	1.34	1.53	2.6
	b (l mg^{-1})	17.1	11.9	29.4
	R^2	0.9578	0.9791	0.9899
Moringa seeds	q_{max} (mg g^{-1})	23.3	42.3	16.1
	b (l mg^{-1})	0.11	0.12	0.1
	R^2	0.9945	0.9901	0.9932

The adsorptive capacities (q_{max}) of all three heavy metals for rice husk in this study is similar, compared to the other reports in literature, including the Langmuir adsorption model (Marshall et al., 1993; Araújo et al., 2010). Rice husk adsorbs 1.75 and 2.74 times more Cu than Zn and Ni, respectively. Maximum sorption capacity ($q_{max,}$, Table 6) suggests the following order for metal ion selectivity for rice husk: Cu > Zn > Ni. In contrast, Zn is adsorbed 1.8 and 1.2 times more than Cu for coconut coir and moringa seeds, respectively. Although Ni is the least adsorbed by coconut coir and moringa seeds, the max adsorption capacities observed using coconut coir and moringa seeds are 4 and 25 times higher than the one obtained for rice husks, respectively. The adsorption selectivity for coconut coir and rice husk is Zn > Cu > Ni.

The adsorption capacities and models (Langmuir) for coconut coir are similar to studies reported in literature. However, in some studies, Ni adsorption capacity (2.51 mg g^{-1}) is higher than adsorption capacity of Zn (1.83 mg g^{-1}) for coconut coir. This may be resulted from the other additional heavy metal ions in the solution or the type/source of the biosorbents used. In multi-element solutions, there may be a decrease in adsorption ability of specific heavy metals due to the competitive adsorption (Sharma et al., 2007). Therefore, adsorption capacity and model comparisons with literature may not be representative since there is no study in literature, reporting the selected mixed heavy metals and metal concentrations without biosorbent modification, similar to our study. Moringa seeds showed the highest adsorption capacity for all heavy metals. However, the binding energies (represented by b) for heavy metals were the highest for rice husk and coconut coir.

In this study, moringa seeds showed approx. an order of magnitude higher adsorption capacities for Cu, Zn and Ni, compared to rice husk and coconut coir, under the same experimental conditions. This may suggest that the functional groups, such as O-H, C-N, N-H and C-O, which moringa seeds contain, play a role during adsorption process by either developing electrostatic forces or complexion between groups and heavy metal ions. Swelam et al (2018) compared the FTIR spectra of the moringa seeds before and after adsorption of lead and observed significant shift or no difference in some peak positions of those functional groups. Similarly, Maina et al (2016) also reported shifts or changes in the peak positions and intensities in the FTIR spectra after heavy metal (lead, cadmium, iron, zinc, magnesium and manganese) adsorption on moringa oleifera tree. The shifting in the peak positions and intensity in the spectra, after lead adsorption, can be a proof for the participation of those specific groups in adsorption process.

In addition to this, cation selectivity of a biosorbent can be influenced by electrostatic attraction (influenced by hydrated radius), cation charge and enthalpy of hydration and

complex and precipitate formation (Hendricks, 2016). Effects of cation charge and complex and precipitate formation were dismissed as all metals are divalent (same charge) and experiments were performed at pH 6 to prevent the influence of precipitation. Surface charges of the biosorbents are negative and in the same region for all biosorbents. Therefore, the percentage of removal for metal ions may also be explained by the difference in hydrated radius. Reports in literature show that in general, the greater the atomic weight, electronegativity, and ionic size, the greater will be the affinity for sorption (Mattuschka and Straube, 1993). Among the metals tested, Cu (0.419 nm) and Zn (0.430 nm) (Ouki and Kavannagh, 1997; Oter and Akcay, 2007) present larger ionic radius and hence higher adsorption capacity unlike the Ni (0.404 nm) (Mobasherpour et al., 2012), which presents lower adsorption capacity (Araújo et al., 2010).

Conclusion

We demonstrated the successful removal of Cu, Zn and Ni from contaminated water, using rice husk, coconut coir and moringa seeds. without modification. For the first time, the performance of these biosorbents were analysed under the same conditions. Heavy metals were removed up to 99% using 40 g l^{-1} biosorbents at pH 6, without precipitation. The highest adsorption capacities (Cu= 23.3 mg g^{-1}, Zn= 42.3 mg g^{-1} and Ni= 16.1 mg g^{-1}) were observed using moringa seeds, followed by rice husk and coconut coir. Adsorption isotherms and kinetics fitted Langmuir and Pseudo-second order models for all biosorbents.

Acknowledgments

Begum Tokay thanks to University of Nottingham, Faculty of Engineering for financial support. The authors thank the Nanoscale and Microscale Centre (nmRC) for providing access to characterisation instruments. We thank Dr Athil Al-Shihabi Al-Ani and Mrs Tasneem Muhammed for FTIR and XRF characterisations, respectively.

Appendix A. Supplementary Materials

Supplementary Data.

References

Abdullah, N., Yusof, N., Lau, W.J., Jaafar, J., Ismail, A.F. 2019. Recent trends of heavy metal removal from water/wastewater by membrane technologies. J. Ind. Eng. Chem., 76, 17-38.

Abdulkarim, S. M., Long, K., Lai, O. M., Muhammad, S. K. S, and Ghazali, H. M. 2005. Some physico-chemical properties of Moringa oleifera seed oil extracted using solvent and aqueous enzymztic methods. Food Chem., 93, 253–263

Ahmaruzzaman, M., Gupta, V.K. 2011. Rice Husk and Its Ash as Low-Cost Adsorbents in Water and Wastewater Treatment. Ind. Eng. Chem. Res, 50(24), 13589-13613.

Araújo, S.T., Alves, V.N., Rezende, H.C., Almeida, L.S., De Assunçâo, R.M.N., César, R., Tarley, T., Segatelli, M.G., and Coelho, N.M.M. 2010. Characterization and use of Moringa oleifera seeds as biosorbent for removing metal ions from aqueous effluents. Water Sci. Tech, 62, 2198-2203.

Aravind, C. Pradesh, V.A., and Mahindra, I.A. 2017. Removal of heavy metals from industrial wastewater using coconut coir, Int. J Civil Eng Tech, 8, 1869-1871.

Asim, N., Amin, M.H., Samsudin, N.A., Badiei, M., Razali, H., Akhtaruzzaman, M., Amin, N., Sopian, K. 2020. Development of effective and sustainable adsorbent biomaterial from an agricultural waste material: Cu(II) removal. Mater. Chem. Phys., 249, 123-128.

Bakker, K. 2012. Water Security: Research Challenges and Opportunities. Science, 337(6097), 914-915.

Bhatti, H.N., Mumtaz, B., Hanif, M.A., Nadeem, R. 2007. Removal of Zn(II) ions from aqueous solution using Moringa oleifera Lam. (horseradish tree) biomass. Process Biochem., 42(4), 547-553.

Blanchard, G., Maunaye, M., and Martin, G. 1984. Removal of heavy metals from waters by means of natural zeolites. Water Res., 18, 1501–1507.

Borba, C.E., Guirardello, R., Silva, E.A., Veit, M.T., Tavares, C.R.G. 2006. Removal of nickel(II) ions from aqueous solution by biosorption in a fixed bed column: experimental and theoretical breakthrough curves. Biochem. Eng. J., 30, 184-191.

Douven, S., Paez, C.A., and Gommes, C.J., 2015. The range of validity of sorption kinetic models. J. Colloid Interface Sci., 448, 437-450.

Farrokhzadeh, H., Taheri, E., Ebrahimi, A., Fatehizadeh, A., Dastjerdi, M., Bina, B. 2013. Effectiveness of Moringa oleifera powder in removal of heavy metals from aqueous solutions. Fresenius Environ. Bull., 22(5a), 1516-1523.

Fu, F. and Wang, Q. 2011. Removal of heavy metal ions from wastewaters: A review. J. Environ. Manage., 92(3), 407-418.

Garcia-Fayos, B., Arnal, J.M., Piris, J., and Sancho, M. 2016. Valorization of Moringa oleifera seed husk as biosorbent: isotherm and kinetics studies to remove cadmium and copper from aqueous solutions. Desalination Water Treatment, 57, 23382-23396.

Guo, H., Zhang, S., Kou, Z., Zhai, S., Ma, W., Yang, Y. 2015. Removal of cadmium(II) from aqueous solutions by chemically modified maize straw. Carbohydr. Polym., 115, 177-185.

Gupta, V.K., Nayak, A. 2012. Cadmium removal and recovery from aqueous solutions by novel adsorbents prepared from orange peel and Fe_2O_3 nanoparticles. Chem. Engin. J., 180, 81-90.

Hendrawati, Yuliastri, I.R., Nurhasni, Rohaeti, E., Effendi, H., Darusman, L.K. 2016. The use of Moringa Oleifera Seed Powder as Coagulant to Improve the Quality of Wastewater and Ground Water. IOP Conf. Ser.: Earth and Environ. Sci., 31, 012033.

Hoffland Environmental, I. Hydroxide Precipitation of Metals, Vol. 2020 https://heienv.com/hydroxide-precipitation-of-metals/ (last accessed 09 May 2021).

Kadirvelu, K., Namasivayam, C. 2003. Activated carbon from coconut coirpith as metal adsorbent: adsorption of Cd(II) from aqueous solution. Adv. Environ. Res. 7(2), 471-478.

Kalavathy, M.H. and Miranda L.M. 2010. Moringa oleifera—A solid phase extractant for the removal of copper, nickel and zinc from aqueous solutions. Chemical Engineering Journal, 158, 188-199.

Kołodyńska, D., Krukowska, J., Thomas, P. 2017. Comparison of sorption and desorption studies of heavy metal ions from biochar and commercial active carbon. Chem. Engin. J., 307, 353-363.

Lu, X., Wang, F., Li, X.-y., Shih, K., Zeng, E.Y. 2016. Adsorption and Thermal Stabilization of Pb^{2+} and Cu^{2+} by Zeolite. Ind. Eng. Chem. Res., 55(32), 8767-8773.

Maina, I.W., Obuseng, V., and Nareetsile, F. 2016. Use of Moringa oleifera (Moringa) Seed Pods and Sclerocarya birrea (Morula) Nut Shells for Removal of Heavy Metals from Wastewater and Borehole Water. J Chem, 2016, 1-14.

Marshall, W.E., Champagne, E.T., Evans, W.J. 1993. Use of rice milling by products (hulls & bran) to remove metal ions from aqueous solution. J. Environ. Sei. Health, A28 1992, 1977-1992.

Mattuschka, B., and Straube, G. 1993. Biosorption of metals by a waste biomass. J Chem Tech Biotech, 58, 57-63.

Mobasherpour, I., Salahi, E., and Pazouki, M. 2012. Comparative of the removal of Pb^{2+}, Cd^{2+} and Ni^{2+} by nano crystallite hydroxyapatite from aqueous solutions: Adsorption isotherm study. Arabian J Chem, 5, 439-446.

Mohan, S., and Sreelakshmi, G. 2008. Fixed bed column study for heavy metal removal using phosphate treated rice husk. J. Hazard. Mater., 153(1), 75-82.

Mon, M., Ferrando-Soria, J., Grancha, T., Fortea-Pérez, F.R., Gascon, J., Leyva-Pérez, A., Armentano, D., Pardo, E. 2016. Selective Gold Recovery and Catalysis in a Highly Flexible Methionine-Decorated Metal–Organic Framework. J. Am. Chem. Soc., 138(25), 7864-7867.

O. Bezerra, C., Cusioli, I, L.F., Quesada, H.B., Mantovani, D., , Vieira M.F., and Bergamasco, R. 2020. Assessment of the use of Moringa oleifera seed husks for removal of pesticide diuron from contaminated water. Environ Tech, 41, 191-201.

Obuseng, V., Nareetsile, F., Kwaambwa, H.M. 2012. A study of the removal of heavy metals from aqueous solutions by Moringa oleifera seeds and amine-based ligand 1,4-bis[N,N-bis(2-picoyl)amino]butane. Anal. Chim. Acta, 730, 87-92.

Oter, O. and Akcay, H., 2007. Use of natural clinoptilolite to improve water quality: sorption and selectivity studies of lead(II), copper(II), zinc(II), and nickel(II). Water Environ Res, 79, 329-335.

Oyaro, N., Juddy, O., Murago, E.N.M., Gitonga, E. 2007. The contents of Pb, Cu, Zn and Cd in meat in Nairobi, Kenya. Int. J. Food Agric. Environ., 5, 119-121.

Pathiraja, G.C., De Silva, D.K., Dhanapala, L., and Nanayakkara, N. 2014. Investigating the surface characteristics of chemically modified and unmodified rice husk ash; bottom-up approach for adsorptive removal of water contaminants. Desal Water Treat., 1-10.

Paulino, A.T., Minasse, F.A.S., Guilherme, M.R., Reis, A.V., Muniz, E.C., and Nozaki, J. 2006. Novel adsorbent based on silkworm chrysalides for removal of heavy metals from wastewaters. J. Colloid Interface Sci., 301, 479-487.

Peng, Y., Huang, H., Zhang, Y., Kang, C., Chen, S., Song, L., Liu, D., Zhong, C. 2018. A versatile MOF-based trap for heavy metal ion capture and dispersion. Nat. Commun., 9(1), 187.

Rahim, A.R.A., Johari, I.K., Shehzad, N., Saman, N., and Mat, H. 2021. Conversion of coconut waste into cost effective adsorbent for Cu(II) and Ni(II) removal from aqueous solutions. Environ Eng Res, 26.

Reck, M., Paixão, R.M., Bergamasco, R., Vieira, M.F., and Vieira, A.M.S. 2018. Removal of tartrazine from aqueous solutions using adsorbents based on activated carbon and Moringa oleifera seeds. J Cleaner Production, 171, 85-97.

Rocha, C.G., Zaia, D.A.M., da Silva Alfaya, R.V, and da Silva Alfaya, A.A. 2009. Use of rice straw as biosorbent for removal of Cu(II), Zn(II), Cd(II) and Hg(II) ions in industrial effluents, J Hazardous Mater, 166, 383-388

Rosa, M.F., Medeiros, S.E.S., Malmonge, J.A., Gregorski, K.S., Wood, D.F., Mattoso, L.H.C., and Glenn, G. 2010. Cellulose nanowhiskers from coconut husk fibers: effect of preparation conditions on their thermal and morphological behavior. Carbohydrate Polymers, 81, 83-92.

Sangian, H.F. and Widjaja, A. 2017. Effect of pretreatment method on structural changes of coconut coir dust. Bioresources, 12, 8030-8046.

Seliem, M.K., Komarneni, S., and Abu Khadra, M.R., 2014. Phosphate removal from solution by composite of MCM-41 silica with rice husk: Kinetic and equilibrium studies. Micropore Mesopore Mater., 224, 51-57.

Seliman, A.F., Lasheen, Y.F., Youssief, M.A.E., Abo-Aly, M.M., Shehata, F.A. 2014. Removal of some radionuclides from contaminated solution using natural clay: bentonite. J. Radioanal. and Nucl. Chem., 300(3), 969-979.

Sharma, P., Kumari, P., Srivastava, M.M., Shalini, S. 2007. Ternary biosorption studies of Cd(II), Cr(III) and Ni(II) on shelled Moringa oleifera seeds. Bioresource Technology, 98, 474-477.

Shukla, S.R., Pai, R.S., and Shendarkar, A.D. 2006. Adsorption of Ni(II), Zn(II) and Fe(II) on modified coir fibres. Separ Purification Tech., 47, 141-147.

Sun, D.T., Peng, L., Reeder, W.S., Moosavi, S.M., Tiana, D., Britt, D.K., Oveisi, E., Queen, W.L. 2018. Rapid, selective heavy metal removal from water by a Metal–Organic Framework/Polydopamine Composite. ACS Cent. Sci., 4(3), 349-356.

Swelam A.A., Sherif, S.S., and Ibrahim, A. 2018. The adsorption kinetics and modelling for Pb(II) removal from synthetic and real wastewater by moringa oleifera seeds. Al Azhar Bulletin of Science, 29, 105-124.

Tariq, M., Durrani, A. I., Farooq, U., and Tariq, M. 2018. Efficacy of spent black tea for the removal of nitrobenzene from aqueous media. J Enviro Management, 223, 771-778.

Tomzcak, F., Sydenstricker, T.H.D., and Satyanarayana, K.G. 2007. Studies on lignocellulosic fibers of Brazil. Part II: Morphology and properties of Brazilian coconut fibers. Composites: Part A, 38, 1710-1721.

World Health Organization, W.H.O 2004. Sulfate in Drinking-water.Vol. 2020.

Zhang, Y., Zheng, R., Zhao, J., Ma, F., Zhang, Y., Meng, Q. 2013. Characterization of H_3PO_4-treated rice husk adsorbent and adsorption of copper(II) from aqueous solution. Biomed Res Int, 2014, 496878-496886.

Supplementary Materials

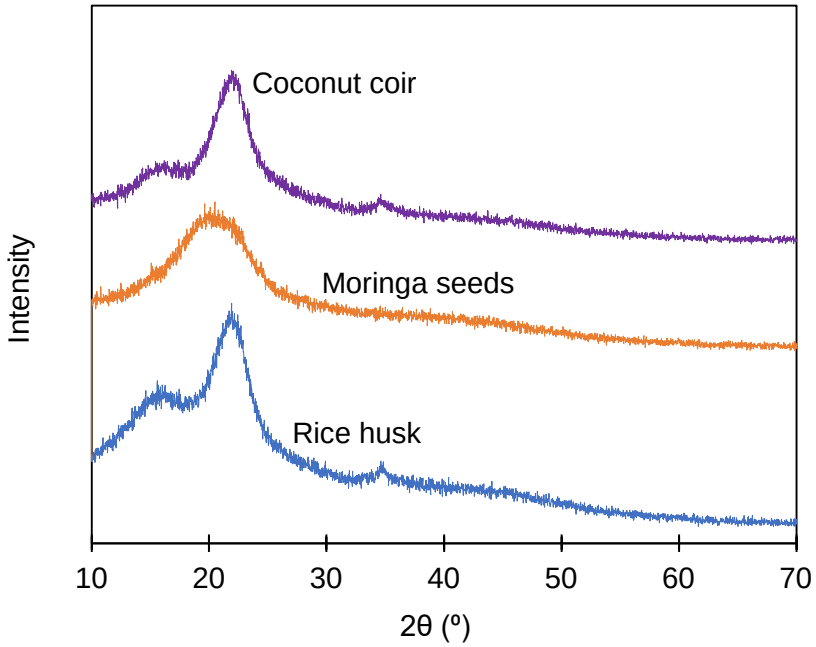

599

600 **Figure S1.** XRD patterns of rice husk, coconut coir and moringa seeds.

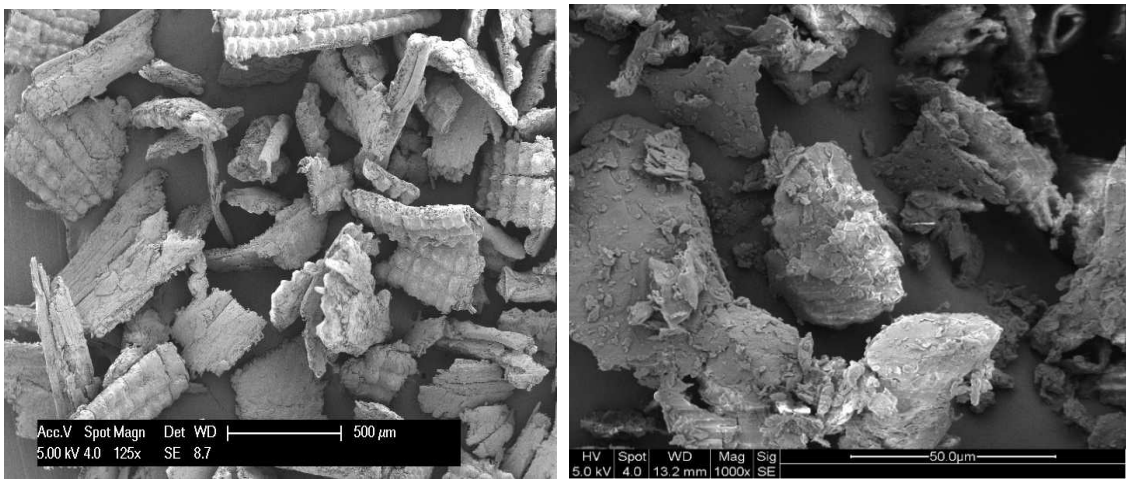

601

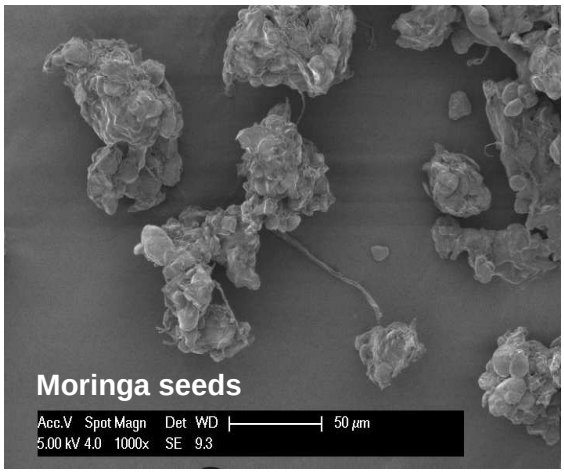

602

603 **Figure S2.** SEM images of rice husk, coconut coir and rice husk.

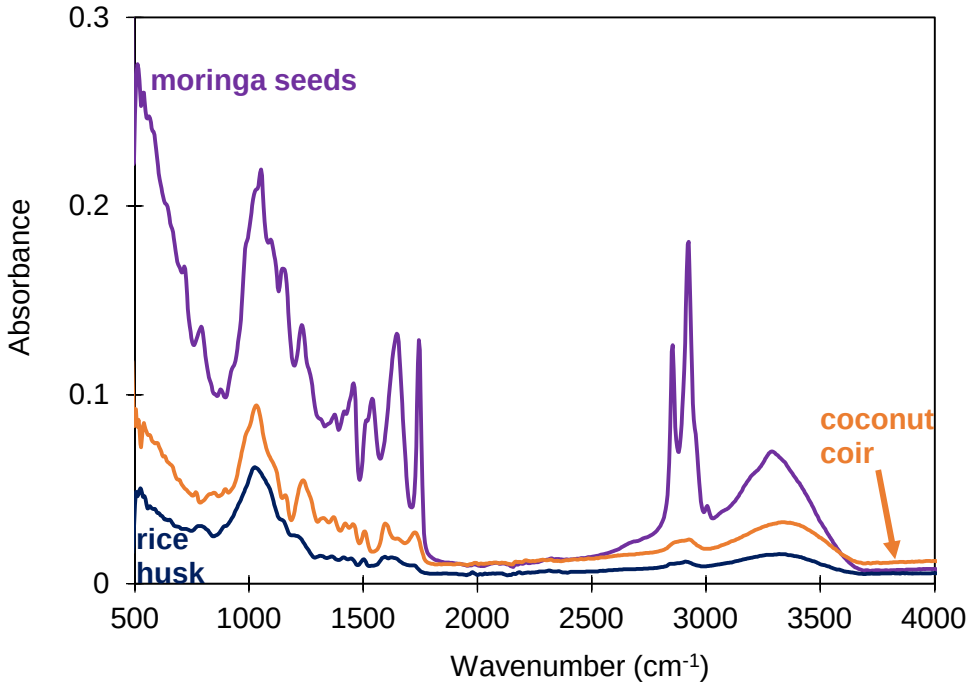

Figure S3. FTIR spectra of rice husk, coconut coir and moringa seeds obtained between 500-4000 cm^{-1}.